1956

Determination of the skin friction drag of a large flat plate of different finishes from boundary layer investigation.

Readdy, Francis Joseph

University of Minnesota

DETERMINATION OF THE SKIN FRICTION DRAG OF A LARGE FLAT PLATE OF DIFFERENT FINISHES FROM BOUNDARY LAYER INVESTIGATION

A Thesis

Submitted to the Graduate Faculty

of the University of Minnesota

by

Francis Joseph Readdy

Lieutenant, United States Navy

In Partial Fulfillment of the Requirements

for the Degree of

Master of Science in Aeronautical Engineering

June 1956

ACKNOWLEDGMENTS

The author wishes to express his appreciation to Professor John D. Akerman for his interest and advice; to Professor Joseph A. Wise for his assistance in programming the data reduction problem for the calculating punch; to Miles Mock for his valuable suggestions and skillful construction of the equipment; to the U. S. Naval Postgraduate School for sponsoring the attendance of the author at the University of Minnesota during this period of study; and to his wife for her encouragement and understanding throughout the entire period of the author's postgraduate study.

F. J. R.

TABLE OF CONTENTS

SYMBOLS

C_F	- Coefficient of total skin friction
F	- Total skin friction force per unit width
L	- Length of test Panel
p	- Pressure
q	- Dynamic pressure
R	- Reynolds number
S	- Area of test panel
T	- Absolute temperature
u	- Streamwise velocity at a point in boundary layer
U	- Streamwise velocity in free stream
x	- Coordinate along surface in direction of flow
y	- Coordinate normal to the surface
δ	- Boundary layer thickness
θ	- Boundary layer momentum thickness
μ	- Coefficient of viscosity
ρ	- Air density

DETERMINATION OF THE SKIN FRICTION DRAG OF A LARGE FLAT PLATE OF DIFFERENT FINISHES FROM BOUNDARY LAYER INVESTIGATION

ABSTRACT

The skin friction drag of a large flat plate employed as the movable panel of a direct force measurement device was determined by means of a boundary layer total pressure survey. Three different surface finishes were investigated in order to determine the effect of surface condition on the skin friction drag and to provide data for the evaluation of the direct force measurement device. The investigation was restricted to turbulent boundary layer in incompressible flow.

The total skin friction force coefficients obtained for a smooth glass plate showed good agreement with the theoretical values for a smooth flat plate. No significant increase in skin friction was found for a polished Alclad surface. A slight increase in skin friction force was indicated as the result of a very limited survey conducted on a painted glass surface. The data obtained from the complete boundary layer surveys were considered satisfactory for use in the evaluation of the direct force measurement device.

DETERMINATION OF THE SKIN FRICTION DRAG OF A LARGE FLAT PLATE OF DIFFERENT FINISHES FROM BOUNDARY LAYER INVESTIGATION

INTRODUCTION

The skin friction drag of a body moving through a real fluid is due to the existence of tangential (shearing) forces in the real fluid causing the fluid to adhere to the body. These tangential forces are associated with a property called viscosity. The adhesion of the particles to the body is known as the condition of no slip. Even for fluids of small viscosity, such as air, because of this condition of no slip there exists a boundary layer through which the fluid velocity varies from that of the wall to that of the free stream.

Within the boundary layer the flow may be laminar, in which the fluid moves in essentially parallel layers, or turbulent, in which the fluid motion is quite disordered. The shearing stress in laminar flow is due to the transfer of downstream molecular momentum between the layers of fluid, while in turbulent flow the momentum transfer is carried out by relatively large masses of fluid as well. Consequently, a turbulent boundary layer produces a greater amount of skin friction drag than does a laminar boundary layer.

Transition from laminar to turbulent boundary layer may be caused by such disturbances as turbulence in the main stream, surface roughness, disturbances imposed within the boundary layer or by shock waves, while the factors affecting transition include

Reynolds number, pressure gradient, Mach number, suction, heat transfer and curvature. For most aircraft surfaces early transition from laminar to turbulent boundary layer occurs and the higher skin friction drag is present. It has recently been estimated (Reference 1) that turbulent skin friction accounts for one half of the total drag of a present day aircraft in cruising flight.

The turbulent boundary layer is composed of three regions (Reference 2) extending from the wall to the free stream:

(1) a very thin region next to the wall, called the laminar sub-layer in which the viscous forces predominate over the inertia forces

(2) a transitional region in which the turbulent shearing stresses are comparable to the viscous stresses, and

(3) the true turbulent region in which the turbulent stresses predominate over the viscous stresses.

No exact solution is known for the turbulent boundary layer, and only approximate methods are available for its solution. The simplest case of a turbulent boundary layer is that existing on a flat plate at zero incidence since the pressure gradient along the wall is zero, and the velocity outside the boundary layer is constant. Several empirical equations have been developed and are in excellent agreement with experimental results (Reference 2). The skin friction of streamlined bodies along which a small pressure gradient exists does not differ greatly from that of the flat plate at zero incidence, provided that

boundary layer separation does not occur. Therefore, the empirical equations developed for the flat plate at zero incidence have widespread use in estimating the skin friction drag of aircraft surfaces.

The empirical equations are applicable only to smooth surfaces, however, and surface roughness has a pronounced effect on skin friction drag. Nikuradse (3) performed extensive experiments on the skin friction of sand roughened pipes. The results were transposed to the case of rough plates by Prandtl and Schlicting (4). These data are expressed as a function of the sand roughness used in the original experiments, however, and application of the data requires that an equivalent sand roughness be determined for the surface condition under consideration. The equivalent sand roughness is a function of grain size, grain shape and how closely the grains are packed. The equivalent sand roughness of painted aircraft surfaces was determined by Young (5), but, in general, it is difficult to express the roughness of aircraft surfaces in these terms.

The effect on skin friction of slightly roughened aircraft surfaces is of increasing importance since a greater percentage of the total aircraft drag in cruising flight is due to skin friction (Reference 1). A more practical approach, perhaps, is the determination of the admissible roughness, i.e., the roughness that can be tolerated without increasing the skin friction drag over that of a smooth surface. This is of particular importance, for it determines the amount of care that must be taken in manufacturing and maintaining an aircraft surface. For

turbulent boundary layers, roughness has no effect and the surface is considered hydraulically smooth if the height of protuberances is less than that of the laminar sub-layer. Schlicting (2) presents considerable data on the admissible height of roughness elements, concluding that the admissible height varies directly with the kinematic viscosity and inversely with velocity. Thus, it can be seen that the surface condition has a profound effect on the skin friction drag and consequently the total drag of a modern aircraft.

The experimental determination of the skin friction drag of a flat plate may be made by measuring the effect of the plate on the air or by measuring the effect of the air on the plate. The former involves the determination of the velocity profile which cannot be obtained directly but must be determined from measurements of other related quantities. The latter involves only the measurement of the movement of a restoring force against which a movable portion of the plate is displaced streamwise under the action of skin friction. The displacement can be calibrated to indicate force.

The purposes of this investigation were to determine the skin friction drag of a large flat plate of different finishes by means of the former method and to provide skin friction drag data for evaluating the results obtained from a direct force measurement investigation conducted concurrently by Wolff (6). This latter purpose greatly dictated the design of the equipment and the procedures that are described in the following sections.

EQUIPMENT

The large flat plate under investigation was that employed in a direct force measurement device designed by Hendley (7) and slightly modified by Wolff (6). A complete description of this apparatus is contained in the above references.

The device consisted of vertically mounted rectangular inner and outer cores of 0.50 inch thick aluminum alloy. The inner core was suspended in the outer core by two parallel piano wires of adjustable length. Test panels, 39.62 inches long, 29.50 inches wide, and 0.25 inches thick were fastened to both sides of the inner core by securing clips mounted on their inner surfaces. Alclad aluminum alloy frame plates of like thickness were attached to the outer core by means of countersunk bolts and were used to frame the test panels. With no force on the test panels, the gaps between the frame plates and the test panels were set at 0.002 inches at the leading edge, 0.010 inches top and bottom, and 0.030 inches at the trailing edge to allow for the rearward movement of the test panels when subjected to drag forces. An electrical circuit was incorporated to provide warning of any contact between the inner and outer cores or between the test panels and the frame plates.

The force measurement device consisted of a pair of cantilever steel springs to which strain gages were attached in such a manner as to record the bending strains. The springs were mounted on the leading edge of the rear member of the outer core. Contact between the inner core and the free end of the cantilever

spring was made by means of an adjustable bolt attached to the trailing edge of the inner core. The change in resistance of the strain gages was readily calibrated in units of force exerted by the drag forces on the test panels.

The complete device was mounted vertically along the centerline of the 38 inch by 5Ø inch test section of the University of Minnesota subsonic wind tunnel. A streamlined wooden nose piece was attached to the leading edge of the device in order to provide as smooth flow as possible on both sides of the one inch thick test apparatus. A sketch of the complete apparatus as installed in the test section is shown in Figure 1.

Two pairs of test panels were used to provide the different surface finishes investigated. One pair consisted of plate glass panels which were tested in their original surface condition and also with the surfaces spray painted with Dupont Duco High Speed Primer Surfacer No. 80 (Red Oxide). The other pair consisted of Alclad sheets, polished by crocus cloth, rotten-stone and jeweler's rouge. These panels were polished smooth to the touch, but many scratches in the surface were visible.

The roughness of samples of the three surface finishes was measured by means of a Brush Surface Analyzer. Typical roughness indications so recorded are shown in Figure 2. The stylus of the Brush Surface Analyzer moves back and forth over a 3/16 inch length of the surface analyzed. As the stylus reverses direction, an abrupt trace is made similar to that caused by a large roughness element. The positions at which the stylus

reversed direction are indicated in Figure 2 by arrows in order to avoid confusing these traces with those caused by surface roughness. Waviness in the plates was examined by means of a machinist's straight edge. None was found in the direction of flow.

The design requirements for the boundary layer total pressure traverse mechanism were:

(a) that it permit boundary layer total pressure profiles to be made at any point on the test panel on either side of the direct force measurement apparatus.

(b) that the pitot tube be positioned rigidly and accurately with respect to the test panel and yet that the method of mounting not mar the finish of the test panel.

(c) that the mechanism be capable of easy relocation from one point on the test panel to any other.

(d) that the boundary layer traverse be controllable from outside the wind tunnel with minimum modification of the wind tunnel test section.

(e) the obvious requirement that the pressure distribution about the mechanism not interfere with the pressure to be measured.

The mechanism shown in Figures 3 and 4 was designed to meet the above requirements. A streamlined probe holder, internally threaded, moved normal to the test panel along a cen-

trally located threaded spindle. Guide rods on either side of the spindle restrained the probe holder against rotation. At the test panel end of the traverse mechanism the guide rods were joined to a streamlined foot. A thin rubber sheeting was glued to the under surface of the foot to prevent marring the test panel finish and to resist movement of the foot relative to the test panel. Two guide rod supports were utilized to promote rigidity. Ball bearings mounted on the foot and the outer guide rod support were utilized as thrust bearings for the spindle. The outer ends of the guide rods were fastened to a mounting bracket which also served as a support for a Selsyn receiver whose shaft was coupled to the outer end of the spindle.

A 0.125 inch brass tube served as the probe stem and was clamped within the probe holder but electrically insulated from it. Provision was incorporated for slight streamwise adjustment. Pressure and electrical leads were connected to the downstream end of the probe stem and were led through holes in the lower guide rod support and the mounting bracket.

The mechanism was clamped to a streamlined strut mounted vertically in the tunnel test section. The pressure lead and the electrical leads to the probe stem and the Selsyn receiver were taped to the trailing edge of this strut and then led downstream along the floor of the test section and out of the tunnel through the pressure equalizing slot. Figure 5 illustrates the method of mounting the boundary layer traverse mechanism. Relocation of the mechanism vertically to another position on the test panel surface was readily accomplished by sliding the mount-

ing bracket and strut clamp along the mounting strut. Relocation of the mechanism to a new longitudinal position also entailed the movement of the mounting strut to the new location. The trailing edge frame plate was not of sufficient width to support the foot of the mechanism while maintaining the desired probe stem length at the trailing edge of the test panels. Therefore, it was necessary to install an additional auxiliary strut, shown in Figure 6, to provide the needed support at this location.

The impact tube was made from 0.035 inch hypodermic tubing whose open end was compressed such that the original 0.022 inch inner diameter was reduced to a height of 0.015 inches. The lower surface was filed to a thickness of 0.002 inches. The cross section of the impact tube is shown in Figure 7.

Traverse of the boundary layer was controlled by a Selsyn transmitter located outside the tunnel, 28 revolutions of the transmitter rotor resulting in a one inch movement of the probe. Movement of the impact tube away from the metallic surface was detected by an ohmmeter connected to the probe electrical lead and to the appropriate portion of the direct force measurement contact warning circuit mentioned previously.

The University of Minnesota subsonic wind tunnel is a return flow type having a closed filleted rectangular test section bled to atmospheric pressure. The static pressure drop between piezometer rings located upstream of the contraction cone and upstream of the test section is measured using a U-tube manometer. Its indication is calibrated with the test section dynamic pressure and then used in regulating the tunnel speed. Static

pressure taps are located at several locations on the top and bottom walls of the test section. The turbulence level of the tunnel has not been determined quantitatively but it is known to be high.

PROCEDURE

The polished Alclad sheets were the first test panels installed. The pressure gradient along the direct force measurement device was determined by means of the static pressure taps located on both sides of the device in the top and bottom walls of the test section. Adjustment of the top and bottom walls of the test section greatly reduced this pressure gradient, but it could not be entirely eliminated at all speeds.

A preliminary investigation was undertaken to determine the effectiveness of various types of distributed roughness elements in causing transition from laminar to turbulent flow. Crepe masking tape and various grades of emery paper were attached to the leading three inches of the wooden nose piece of the test apparatus. Boundary layer total pressure surveys were made at one position on the leading edge frame plate at various speeds throughout the desired speed range. Turbulent profiles were obtained for each of the roughnesses at all the speeds. The transitioning method of least roughness, crepe masking tape, was then selected in order to minimize the profile distortion described by Klebanoff and Diehl (8).

At the trailing edge of the test panel, boundary layer total pressure traverses were conducted at the centerline and at points three inches from the top and bottom of the panel. The traverses were made by placing the impact tube on the test panel surface, setting the desired tunnel speed and measuring the total pressure on the surface. Counterclockwise rotation of the Selsyn transmitter rotor moved the impact tube away from the panel surface, the exact breakaway point being detected by

the ohmmeter. Total pressure measurements were recorded at intervals through the boundary layer until no further increase in total pressure could be detected. The test section static pressure and the barometric pressure were recorded during each traverse. Wet and dry bulb temperatures were taken at the beginning and end of each traverse by inserting thermometers into the pressure equalizing slot. Traverses were made at four tunnel velocities: 64, 143, 231 and 286 feet per second.

The boundary layer traverse mechanism was then relocated at the leading edge of the test panel. The probe was positioned at the centerline of the panel and the impact tube placed on the surface of the frame plate slightly upstream of the leading edge gap. Boundary layer traverses were made at the four tunnel velocities previously specified. A laminar profile was obtained at the low speed of 64 feet per second at this location, indicating that laminar flow existed over a portion of the test panel at that speed. Therefore, further investigations on the Alclad panels were conducted only at the three higher velocities which resulted in turbulent flow over the entire surface of the test panels. In addition to those at the centerline, boundary layer traverses were made at points three inches from the top and bottom of the panel at the leading edge using the same technique described previously. Identical procedure was followed for the test panel on the other side of the direct force measurement apparatus.

The polished Alclad test panels were removed and the plate glass panels installed. Since it was desirable to obtain

low speed turbulent flow data, 3M No. 150 emery paper was substituted for the crepe masking tape on the leading portion of the nose piece in order to insure transition at that location. Boundary layer traverses were made on both sides at the same locations described for the Alclad panels. Identical procedure was employed with the exception of the technique used to determine the point at which the impact tube left the panel surface. Since the electrical circuit could not be used, the breakaway point was recorded as that at which an increase in the total pressure was detectable. Turbulent profiles were obtained at the leading and trailing edges of the glass panels at all four tunnel speeds.

The plate glass panels were spray painted while installed in the direct force measurement device. A complete investigation of the painted glass panels was precluded by the lack of time available. Therefore, boundary layer measurements were made only at the centerline on one side of the device. The procedure used was the same as that described for the glass plates.

RESULTS AND DISCUSSION

The total skin friction force acting on a unit width of the test panel was calculated by applying the von Karman momentum relation between the leading and trailing edges at the three vertical locations investigated on each side of the device. Sample calculations are shown in the Appendix. In order to provide comparison data for Wolff (6) in his evaluation of the direct force measurement device, the average value of skin friction force per unit width was determined for each surface finish. The coefficient of total skin friction and the Reynolds number based on the test panel length as the characteristic length were computed. These results are shown in Figure 8.

In order to compare the skin friction force results with existing theory it was necessary to determine if the conditions under which the investigation was made approximated those assumed in the theoretical analysis; i.e., a smooth flat plate at zero incidence, with no pressure gradient, and turbulent boundary layer existing from the leading edge. The glass plate was assumed to best approximate the smooth plate.

The roughness trace shown in Figure 2a indicated an average roughness element height of approximately three microinches and was consistent for different locations on the sample tested. The glass plate was considered to by hydraulically smooth. The plates were examined for curvature or waviness in the streamwise direction by means of a machinist's straight edge. None was detected, and the plates were assumed to satisfy the conditions of being flat.

Since the direct force measurement device was mounted along the centerline of the test section, it was assumed that the angle of incidence was near zero. The negative pressure gradient existing along the plate in the streamwise direction was less than three percent of the free stream dynamic pressure. Schlicting (2) points out that the skin friction forces on bodies along which a small negative pressure gradient exists is not materially different from that of a flat plate.

To determine if the boundary layer was fully turbulent, dimensionless velocity distributions were plotted from the boundary layer investigations. They are shown together with the curve of the 1/7 power law turbulent velocity distribution in Figures 9, 10, 11 and 12. The agreement with the theoretical turbulent distribution is excellent at the lowest tunnel speed but lessens with increasing speed, indicating that at the higher speeds the effects of the roughened nose piece had not entirely disappeared. In general, the agreement at the trailing edge was better than at the leading edge, which experienced a greater effect of the roughening elements. The latter result is similar to that described by Klebanoff and Diehl (8) who performed an investigation involving the use of distributed roughness elements to cause transition. The agreement with the theoretical turbulent velocity distribution was considered sufficiently good at all speeds to satisfy the condition of the existence of a fully developed turbulent boundary layer.

Thus, all the conditions required for correlation with existing theory were satisfied except for the condition that the

turbulent boundary layer originate at the leading edge. Therefore, it was necessary to determine for the test panel its virtual origin, defined as the location of the leading edge of a smooth flat plate of equivalent width, having a turbulent boundary layer originating at its leading edge and of sufficient length to develop the same boundary layer conditions as those present at the leading edge of the test panel. The leading edge of the wooden nose piece obviously could not be regarded as the virtual origin because of the favorable pressure gradient existing along the streamlined shape of the nose piece and because of the presence of the roughness elements.

The virtual origin was obtained by computing the length of smooth flat plate required to produce the same boundary layer momentum thickness as the average value of those determined from experimental results at the leading edge of the test panel. The distance, x, from the virtual origin to the leading edge of the test panel was obtained by equating the following relations for the coefficient of total skin friction:

$$C_F = \frac{2\theta}{x}$$

$$C_F = 0.455 \left(\log_{10} R_x\right)^{-2.58}$$

The length from the virtual origin to the trailing edge of the test panel was then used as the characteristic length for Reynolds number calculations. The theoretical total skin friction force per unit width existing from the virtual origin to the leading edge of the test panel was calculated in terms of the boundary layer momentum thickness at the leading edge:

$$F = \rho U^2 \theta$$

This skin friction force was added to that acting on a unit width of the test panel and the coefficient of total skin friction computed using the same characteristic length described above for the Reynolds number computations.

These results for the three surface conditions investigated are plotted in Figure 13. The Schlicting empirical equation is shown for comparison. The agreement of the glass test panels with the empirical skin friction relation is good. The maximum deviation from theory is 4.0 percent and exists at the lowest velocity. With the exception of this point, the agreement is within 2.2 percent and improves with increased velocity.

The lowest tunnel velocity, 64 feet per second, corresponded to a free stream dynamic pressure of only 1.05 inches of alcohol. It was possible to read the alcohol level in the tunnel U tube manometer and in the manometer bank used to measure the static and total pressures only to the nearest 0.05 inches. Therefore, the reading error was on the order of five percent at this velocity. This fact was well recognized prior to the commencement of this investigation, but it was considered desirable to make an investigation at this speed in order to obtain data over as large a Reynolds number range as possible.

The data for the polished Alclad test panels indicate no significant increase in skin friction force coefficients over those obtained for the smooth glass plates. Therefore, the polished Alclad test panels were considered to be hydraulically smooth.

The results for the painted glass panels were obtained from measurements only at the centerline of a single test panel. The skin friction forces obtained from these measurements were compared to those obtained over the corresponding area of the glass plates and the coefficients for the painted glass panels calculated on the basis of their relative values. The results for the painted glass panels at the lowest Reynolds number clearly demonstrate the pressure reading error existing at the lowest tunnel speed, the coefficient for the painted glass surface being five percent less than that for the glass plate. At the intermediate Reynolds numbers the total skin friction coefficients for the painted glass panels exceed those of the glass panels by approximately two percent. At the highest Reynolds number, this excess increases to approximately five percent.

From the roughness traces of the sample surfaces obtained by means of the Brush Surface Analyzer, shown in Figure 2, it would appear that the painted glass surface was not as rough as the polished Alclad panel. However, the painted glass surface was considerably rougher to the sense of touch than the Alclad surface, and it is felt that the roughness of the sample was not truly representative of the painted glass panel roughness. By applying the results of Young (5) to the criteria established by Prandtl and Schlicting (4), the height of the mean geometrical protusions required to cause an increase in skin friction coefficient would be at least 500 microinches, very much greater than that measured for either surface sample. The effect of these protusions would be more pronounced at the higher velocities. It

is possible that the increase in total skin friction coefficient observed for the painted glass panel at the highest velocity indicates this trend. However, because the boundary layer investigation was confined to a limited portion of the painted glass surface, which, itself, may not have been truly representative of the entire surface, the increase in skin friction force over that of the glass plate remains inconclusive.

CONCLUSIONS

From the results of this boundary layer investigation made to determine the skin friction drag of a large flat plate of different finishes and to provide skin friction drag data for evaluating the results of a direct force measurement device, it is concluded that:

(1) The turbulent boundary layer conditions existing over the test panels of the direct force measurement device approximated those existing over a portion of a flat plate at zero incidence.

(2) The total skin friction force coefficients determined for the glass plate test panels showed good agreement with the theoretical values for a smooth flat plate.

(3) No significant increase in skin friction was experienced for a polished Alclad surface under the test conditions investigated, and that surface is considered hydraulically smooth.

(4) No quantitative correlation between the increased skin friction drag of the painted glass surface and its roughness condition is possible because of the inability to correlate the roughness condition of the surface over which the limited boundary layer survey was made with that of the sample as measured by the Brush Surface Analyzer.

(5) The skin friction drag data obtained from complete boundary layer investigations were satisfactory for use in evaluating the results of the direct force measurement device.

APPENDIX

CALCULATIONS

The following data were recorded during each boundary layer traverse. Sample calculations are performed for the glass plate at a free stream velocity of 231 feet per second.

p_B - barometric pressure, inches of mercury

$p - p_B$ - difference between test section static pressure and barometric pressure, inches of alcohol

q - dynamic pressure, difference between total pressure and static pressure, inches of alcohol

y' - distance traversed by the probe normal to the surface measured from its surface position, shaft revolutions.

t_D - dry bulb temperature in tunnel, degrees Fahrenheit

t_W - wet bulb temperature in tunnel, degrees Fahrenheit.

The conversion factors necessary for calculations are:

1 in. alcohol = 0.0595 in. Hg. = 4.21 lbs./ft.^{2}

1 revolution = 0.0357 in. = 0.002976 ft.

Calculation of Density

The static pressure in the test section in inches of mercury was determined:

$$p = p_B + (p - p_B)$$

$$p = 29.22 + (0.95)(0.0595)$$

$$p = 29.28 \text{ in. Hg.}$$

The average value of the wet and dry bulb temperatures were obtained from the readings taken at the commencement and completion of each traverse:

$$t_D = 88^\circ \text{ F}$$

$$t_W = 69^\circ \text{ F}$$

Entering the Air Density Tables (Reference 9) with the values of pressure and temperature:

$$\rho = 0.07051 \text{ lbs./ft.}^3 = 0.00219 \text{ slugs/ft.}^3$$

Calculation of Velocity

The velocity was determined from the value of dynamic pressure recorded and the value of density computed above:

$$U = \sqrt{\frac{2q}{\rho}}$$

$$U = \sqrt{\frac{(2)(13.90)(4.21)}{0.00219}}$$

$$U = 231 \text{ ft./sec.}$$

Calculation of Reynolds Number

The coefficient of viscosity was determined from Sutherland's formula:

$$\mu = 2.270 \frac{T^{3/2}}{T + 198.6} \times 10^{-8} \text{ for } T = 548^\circ \text{ R}$$

$$\mu = \frac{(2.270)(548)^{3/2}}{746.6} \times 10^{-8}$$

$$\mu = 39.0 \times 10^{-8} \text{ lb.sec./ft.}^2$$

The Reynolds number based on the test panel length, L, was then:

$$R_L = \frac{\rho UL}{\mu} \text{ where } L = 3.30 \text{ ft.}$$

$$R_L = \frac{(0.00219)(231)(3.30)}{39.0 \times 10^{-8}}$$

$$R_L = 4{,}281{,}000$$

Calculation of Skin Friction

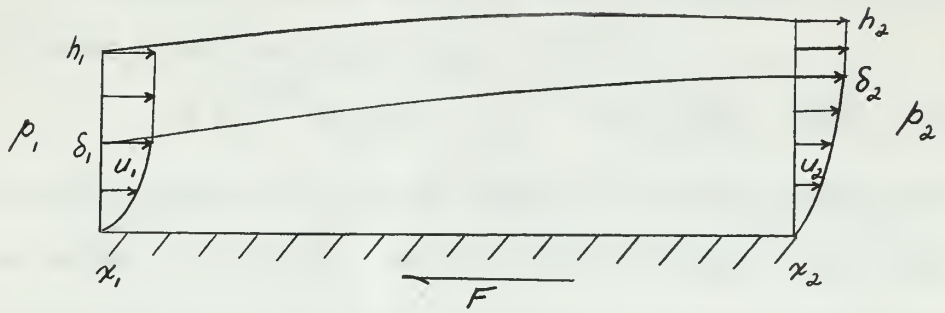

Consider a region in steady two dimensional incompressible flow bounded by perpendiculars to the test panel at its leading and trailing edges, by the panel itself, and by an arbitrary streamline existing completely outside the boundary layer. Denoting the perpendicular distance from the panel to the streamline as h, and using the subscripts 1 and 2 to indicate the leading and trailing edges, respectively, the forces per unit width acting parallel to the surface of the plate (downstream positive) may be summed up as follows:

(a) The skin friction of the plate, -F

(b) The difference in the forces exerted by the pressures at the ends, $p_1h_1 - p_2h_2$

(c) The pressure existing in the free stream acting on the vertical projection of the streamline, approximated by the expression,

$$\frac{p_1 + p_2}{2}(h_2 - h_1) = (p_1 + \frac{\Delta p}{2})(h_2 - h_1)$$

(d) The momentum loss, $\int_0^{h_1} \rho_1 u_1^2 dy_1 - \int_0^{h_2} \rho_2 u_2^2 dy_2$

where u represents the streamwise velocity both within the boundary layer and in the free stream.

The skin friction drag may then be expressed in terms of the other forces and simplified to the form:

$$F = \int_0^{h_1} \rho_1 u_1^2 dy_1 - \int_0^{h_2} \rho_2 u_2^2 dy_2 \quad \frac{\Delta p(h_1 + h_2)}{2}$$

The only unknowns on the right hand side of this equation are the values of h_1 and h_2. Subject to the condition stated above that h_1 and h_2 be outside of the boundary layer, an arbitrary value of h_1 may be chosen and the equation of continuity applied to the flow bounded by the wall and the streamline between the leading and trailing edges:

$$\int_0^{h_1} \rho_1 u_1 dy_1 = \int_0^{h_2} \rho_2 u_2 dy_2$$

Each side of this equation may be divided into two integrals; one extending from the wall to the outer edge of the boundary layer where the velocity equals that of the free stream, designated as $y = \delta$, and the other extending from that point to the streamline, h. Since the value of u is independent of y outside the boundary layer, the equation of continuity reduces to

$$\int_0^{\delta_1} \rho_1 u_1 dy_1 + \rho_1 U_1 (h_1 - \delta_1) = \int_0^{\delta_2} \rho_2 u_2 dy_2 + \rho_2 U_2 (h_2 - \delta_2)$$

Since $q = \frac{\rho u^2}{2}$, $u = \sqrt{\frac{2q}{\rho}}$, and the equation can be reduced to the form

$$\rho_1^{\frac{1}{2}} \int_0^{\delta_1} q_1^{\frac{1}{2}} dy_1 + \rho_1^{\frac{1}{2}}(h_1 - \delta_1) = \rho_2^{\frac{1}{2}} \int_0^{\delta_2} q_2^{\frac{1}{2}} dy_2 + \rho_2^{\frac{1}{2}} q_2 (h_2 - \delta_2)$$

To evaluate the integral, a smooth curve was drawn through the experimental data points and the function q(y) obtained at regular intervals in order to apply Simpson's approximation.

Because 100 Boundary layer traverses had been made in the investigation, over 3,000 profile points were required for the solution of the continuity equation alone. Since repetitious use of these points was necessary for the evaluation of the momentum integrals, and the calculation of the boundary layer momentum thickness to determine the virtual origin, the data reduction was programmed for solution on the University of Minnesota I.B.M. Model 602A Calculating Punch.

BIBLIOGRAPHY

1. Oswald, W. Bailey: Applied Aerodynamics and Flight Mechanics. Journal of Aeronautical Sciences, Vol. 23, No. 5, May 1956.

2. Schlicting, H.: Boundary Layer Control. McGraw-Hill Book Co. Inc., 1955.

3. Nikuradse, J.: Strömungsgesetze in rauhen Rohren. Forschg.-Arb. Ing.-Wesen No. 361, 1933.

4. Prandtl, L. and Schlicting, H.: The Resistance Law for Rough Plates. (Werft-Reederei-Hafen, 1934) U. S. Navy Dept., David W. Taylor Model Basin, Transl. 258, 1955.

5. Young, A. D.: The Drag Effects of Roughness at High Sub-critical Speeds. J. Roy. Aero. Soc., 1950.

6. Wolff, J. M.: An Evaluation of Equipment To Measure Directly The Skin Friction Forces on A Flat Plate. M. S. Thesis, University of Minnesota, May 1956.

7. Hendley, A. C.: Study of Optimum Gains in Skin Friction Coefficient in Turbulent and Laminar Flow for Different Qualities of Aircraft Finishes and Design and Construction of Test Apparatus, M. S. Thesis, University of Minnesota, August 1955.

8. Klebanoff, P. S. and Diehl, Z. W.: Some Features of Artificially Thickened Fully Developed Turbulent Boundary Layers With Zero Pressure Gradient. NACA TN 2475, 1951.

9. Boehnlein, Charles T.: Air Density Tables. University of Minnesota Engineering Experiment Station Technical Paper No. 17.

10. Von Kármán, Th.: On Laminar and Turbulent Friction. NACA TM 1902, 1946.

11. Bidwell, Jerold M.: Application of the von Kármán Momentum Theorem to Turbulent Boundary Layers. NACA TN 2571, 1951.

12. Dhawan, S.: Direct Measurement of Skin Friction. NACA Report 1121, 1953.

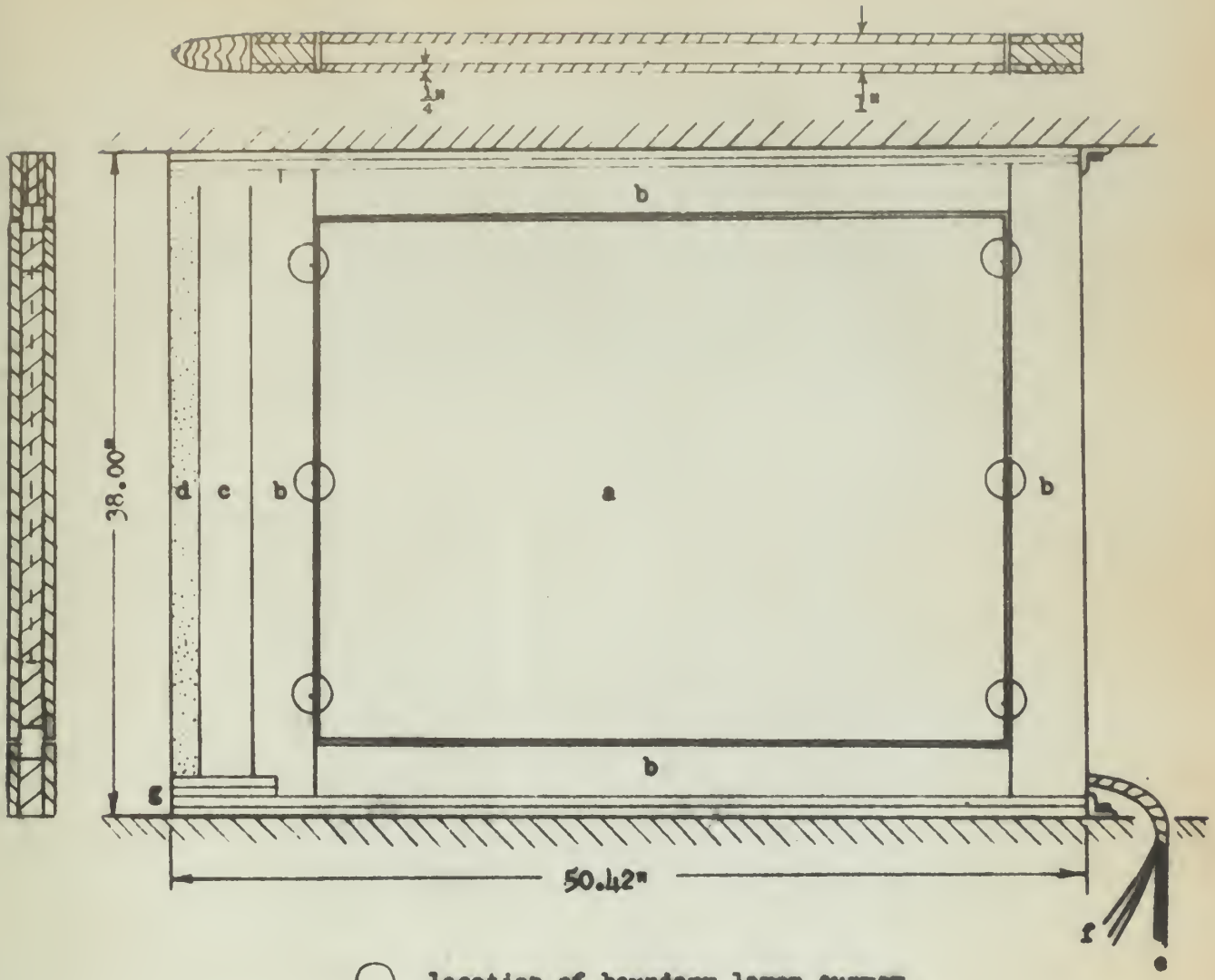

◯- location of boundary layer survey

a - test panel - 39.62 x 29.5 in.

b - frame plates

c - wooden nose piece

d - #150 emery paper

e - pressure leads

f - strain gage leads

g - masking tape

flow direction from left to right

Figure 1

Direct Force Measurement Device

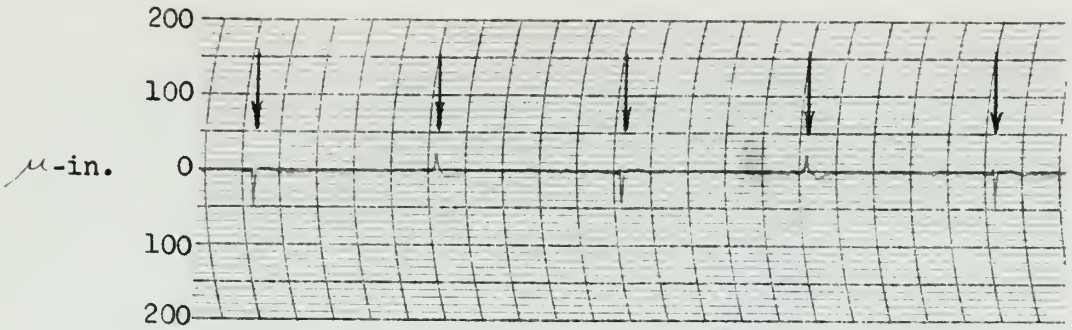

a - glass

b - painted glass

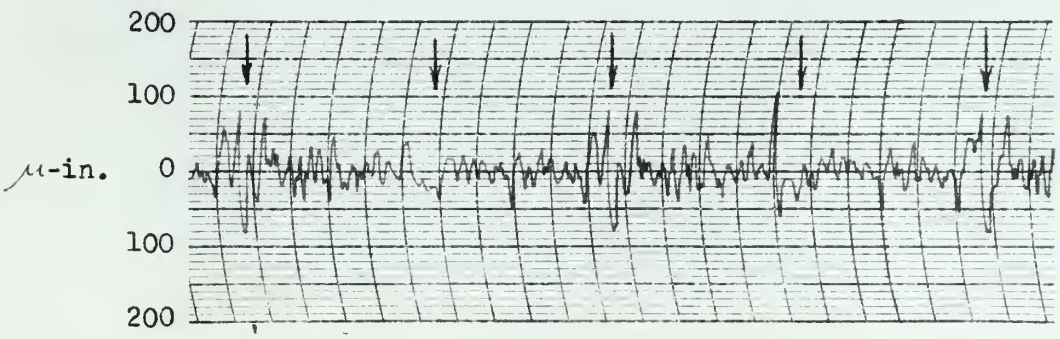

c - polished Alclad

Figure 2

Surface Roughness Traces of Samples Measured

by Brush Surface Analyzer

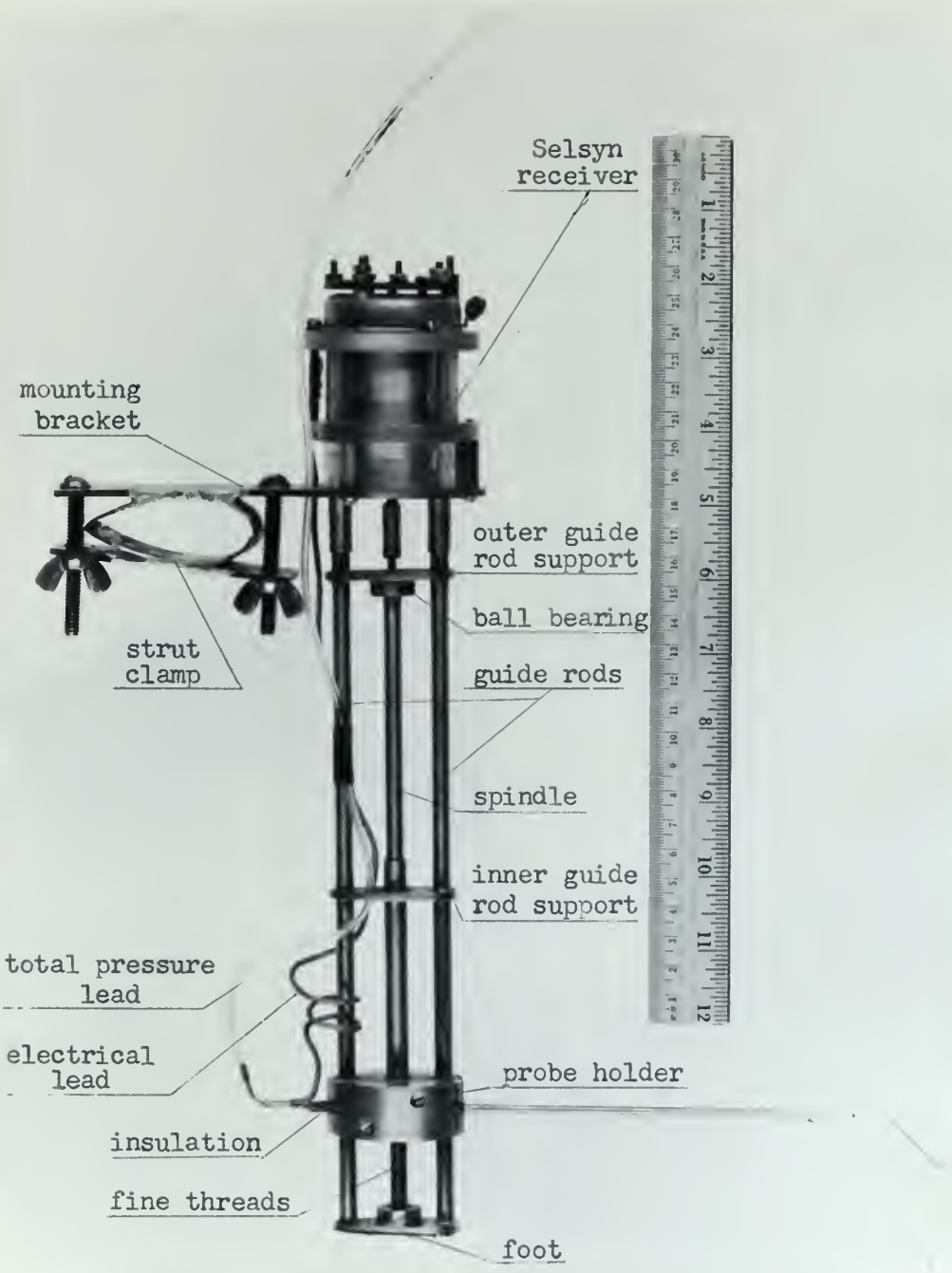

Figure 3

Boundary Layer Traverse Mechanism

(Probe tip not included)

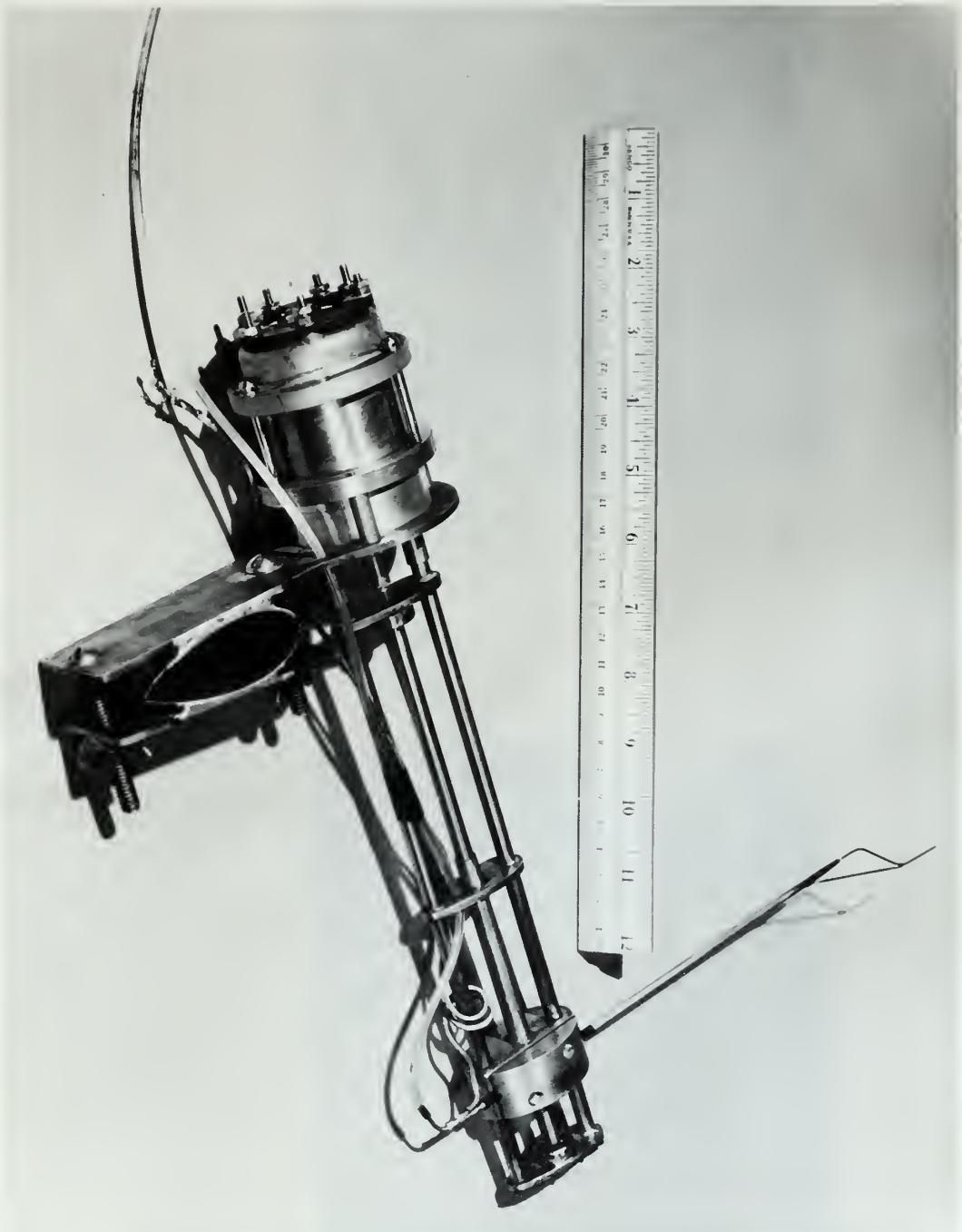

Figure 4

Boundary Layer Traverse Mechanism

(Including probe tip)

a. View from contraction cone
(Glass panel shown)

b. View from test section
(Painted glass panel shown)

Figure 5

Mounting of Boundary Layer Traverse Mechanism

a. View from outside the tunnel test section

b. Close-up

Figure 6

Mounting of Boundary Layer Traverse Mechanism at Trailing Edge of Test Panel

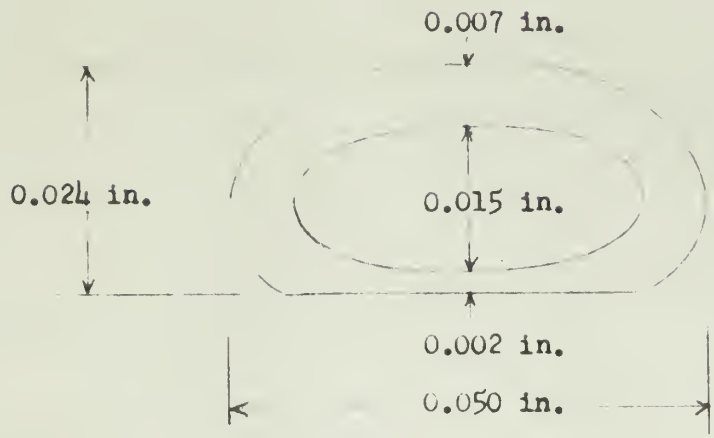

Figure 7

Impact Tube Opening

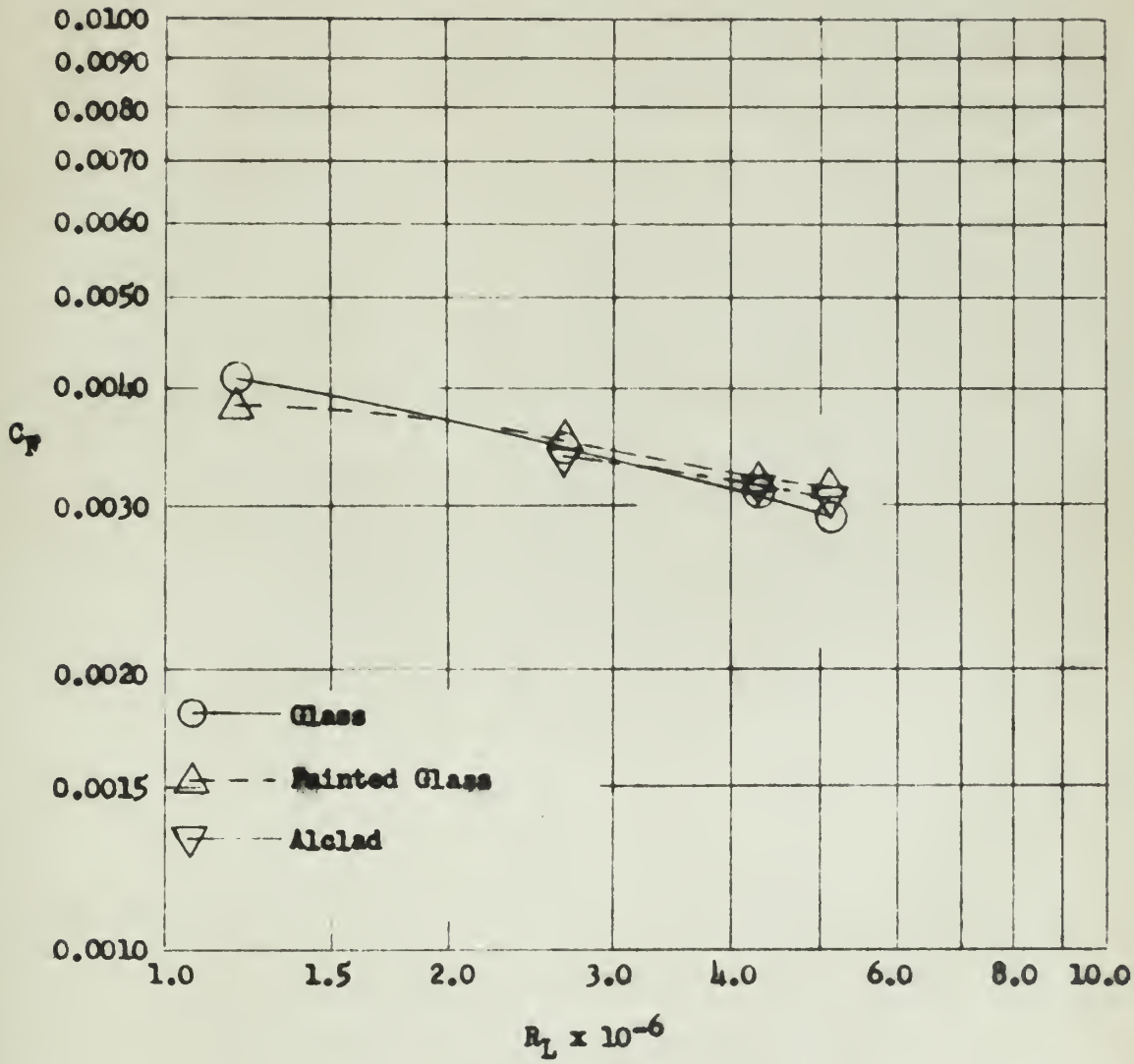

Figure 8

Variation of total skin friction coefficient with Reynolds Number based on test panel length

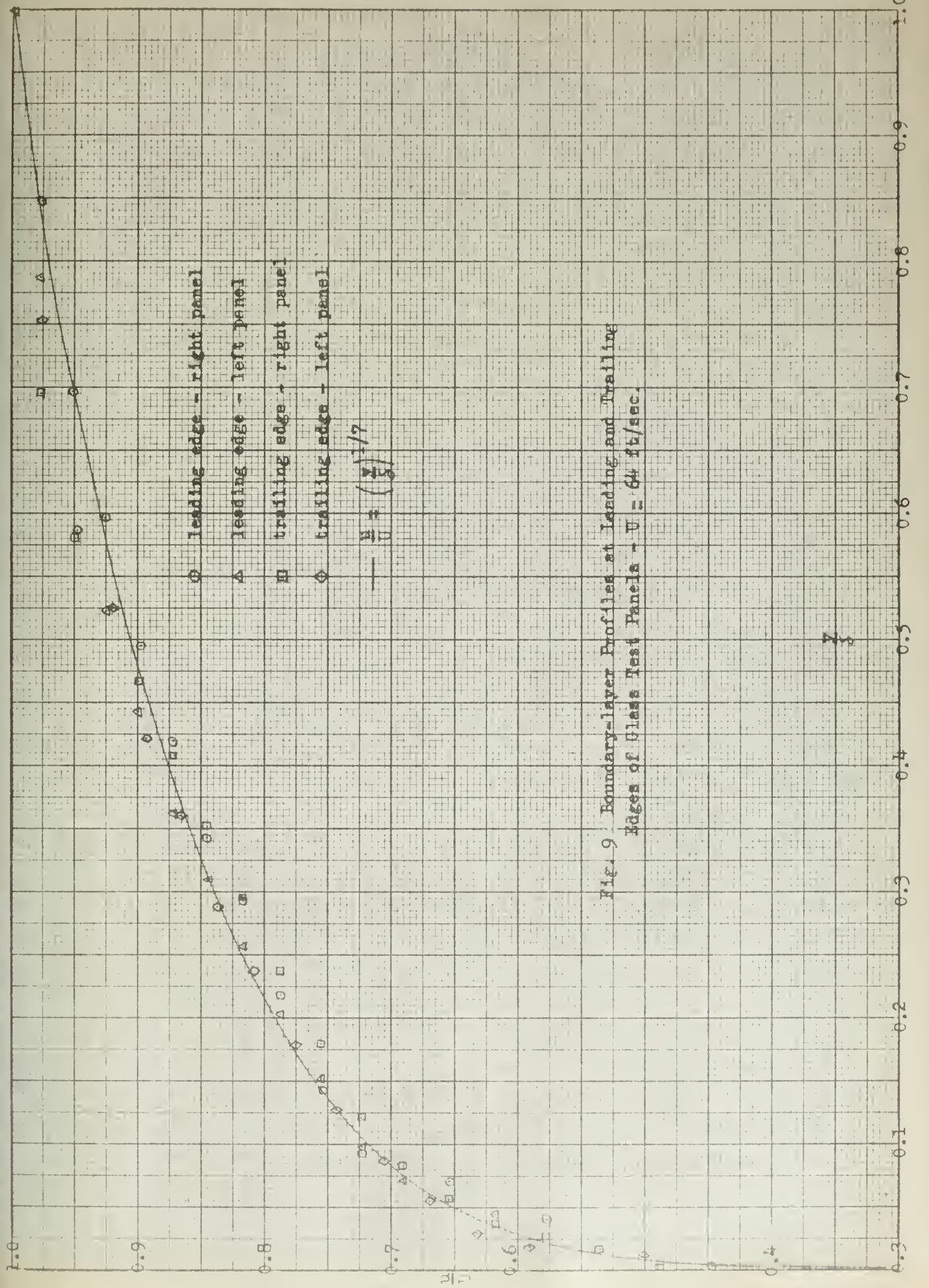

Fig. 9 Boundary-layer Profiles at Leading and Trailing Edges of Glass Test Panels - U = 64 ft/sec.

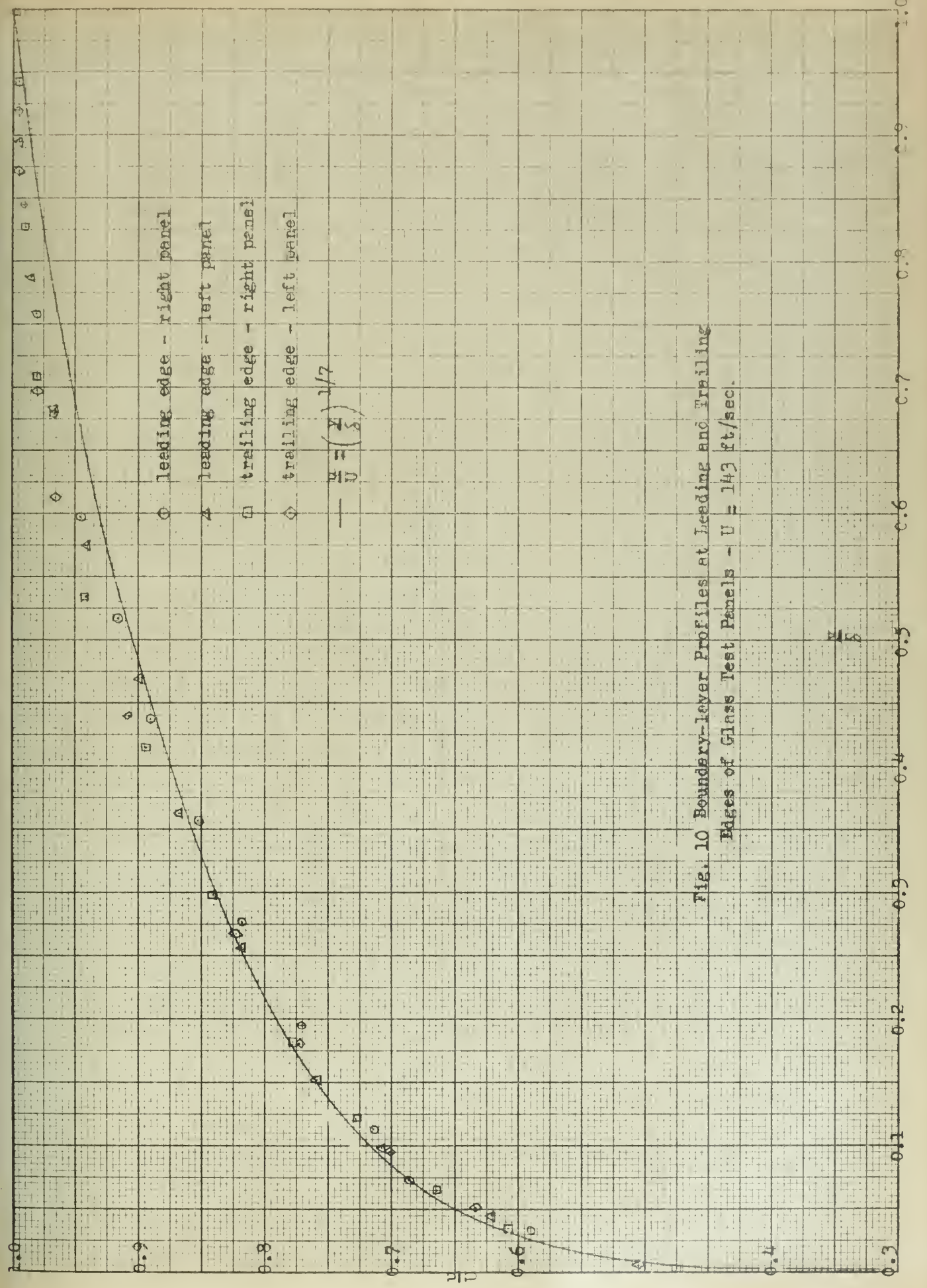

Fig. 10 Boundary-layer Profiles at Leading and Trailing Edges of Glass Test Panels - U = 143 ft/sec.

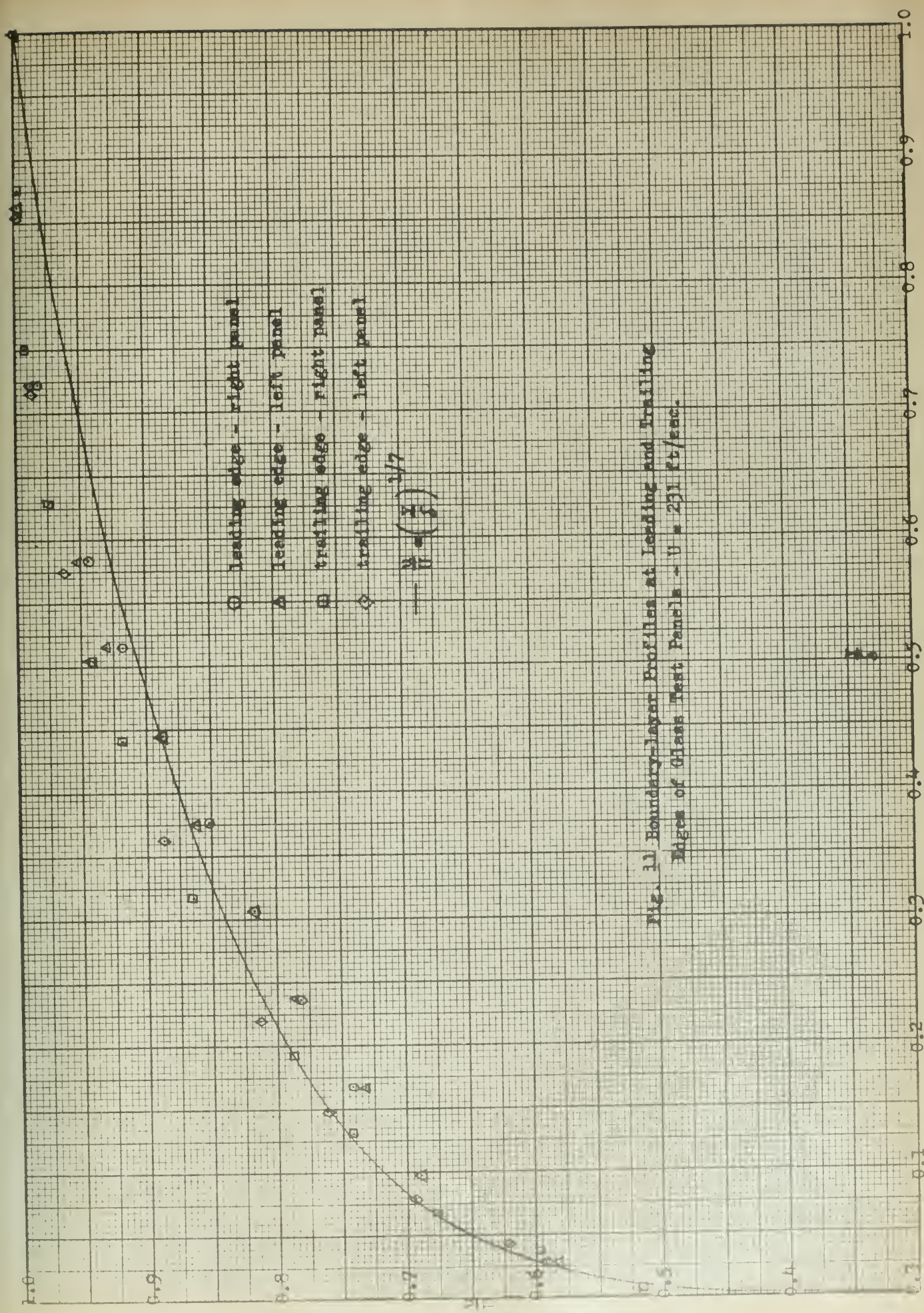

Fig. 11 Boundary-layer Profiles at Leading And Trailing Edges of Glass Test Panels - U = 231 ft/sec.

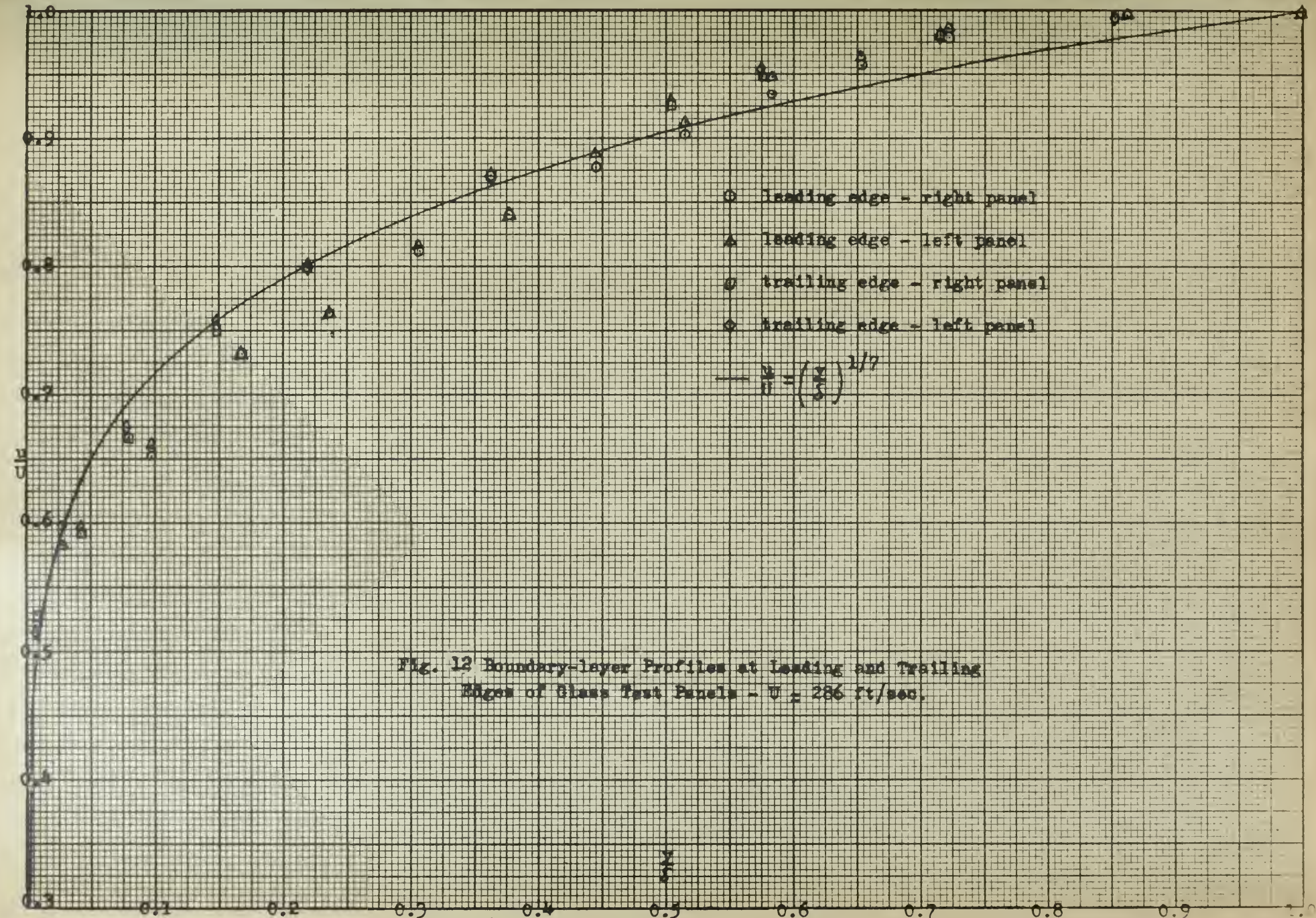

Fig. 12 Boundary-layer Profiles at Leading and Trailing Edges of Glass Test Panels - U_∞ = 286 ft/sec.

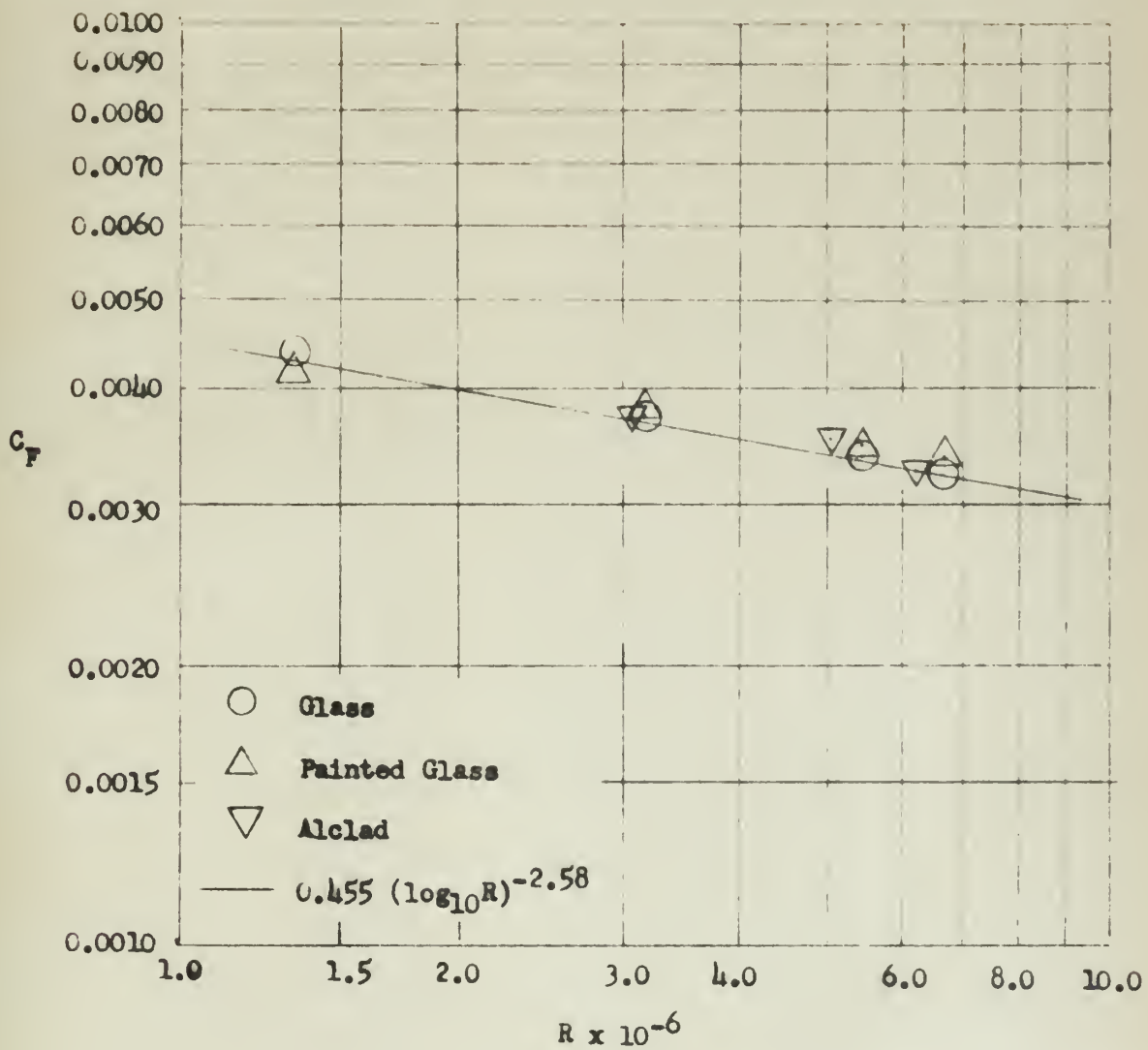

Figure 13

Variation of total skin friction coefficient with Reynolds Number